

Supplementary Information

Zinc oxide nanocrystals as nano-antibiotic and osteogenic/osteoinductive agents

Nadia Garino¹, Pasquale Sanvitale¹, Bianca Dumontel¹, Marco Laurenti¹, Montserrat Colilla^{2,3}, Isabel Izquierdo Barba^{2,3}, Valentina Cauda^{1*}, Maria Vallet-Regí^{2,3*}

¹ Department of Applied Science and Technology, Politecnico di Torino, Corso Duca degli Abruzzi 24, 10129 Turin, Italy;

² Departamento de Química en Ciencias Farmacéuticas, Facultad de Farmacia, Universidad Complutense de Madrid, Plaza Ramón y Cajal s/n, 28040 Madrid, Spain.

³ Networking Research Center on Bioengineering, Biomaterials and Nanomedicine (CIBER-BBN), Madrid, Spain

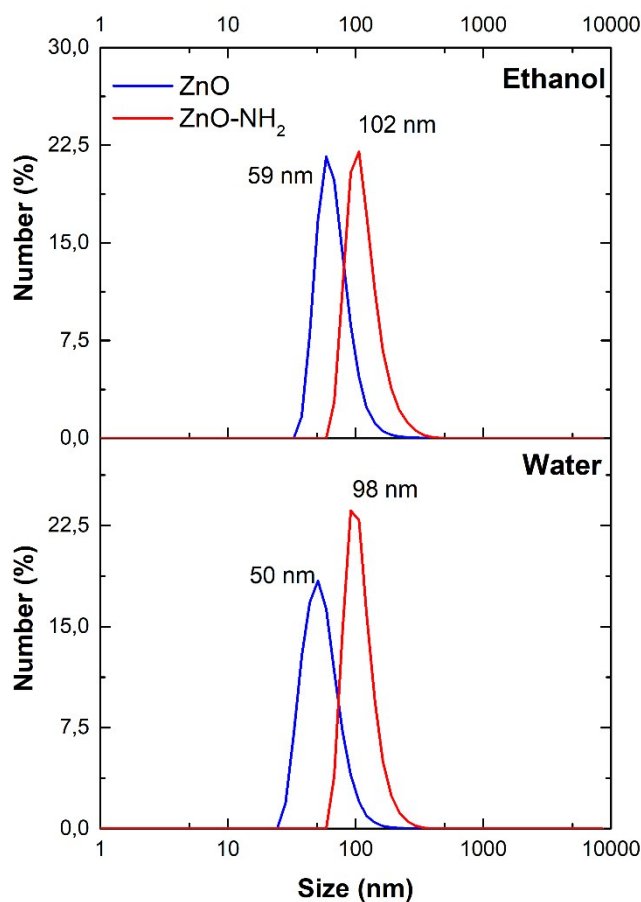


Figure S1. Size distribution curves deriving from Dynamic Light Scattering (DLS) measurements for ZnO and ZnO-NH₂ NCs in Ethanol (top) and water (bottom)

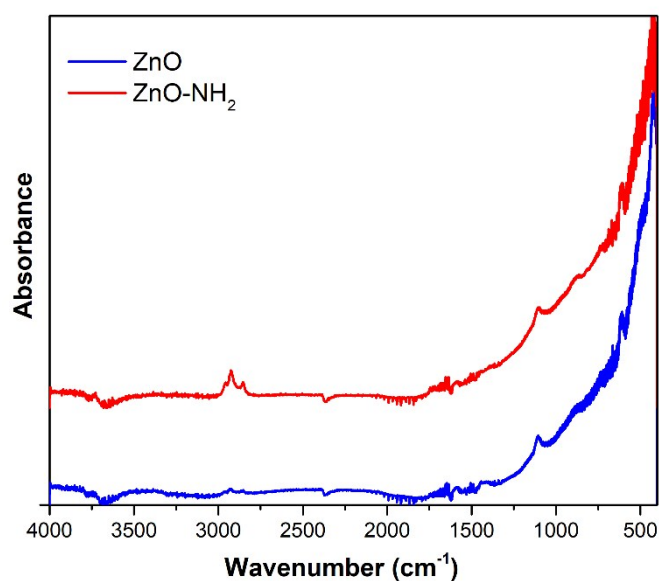


Figure S2. Fourier Transform Infra-Red (FT-IR) spectra of ZnO and ZnO-NH₂ NCs

The FT-IR spectra (Figure S2) of ZnO and ZnO-NH₂ nanocrystals show both an intense mode at 440 cm⁻¹ typical of Zn-O vibration. In addition, the two spectra show, with different intensities, the symmetric and antisymmetric stretching of -CH₂ and -CH₃ groups at 2860 and 2925 cm⁻¹, respectively. These vibrations are attributed to residual acetate groups on the ZnO surface due to the precursors used in the synthetic procedure. However, in the case of ZnO-NH₂ NCs, the 2860 and 2925 cm⁻¹ stretching modes are more intense because of the presence of the propyl chain of the amine-functional group, thus confirming the successful functionalization of the ZnO surface.

Moreover, the broad band from 3600 to 3400 cm⁻¹, due to the stretching vibrations of hydroxyl groups on the ZnO surface, are less pronounced in the ZnO-NH₂ sample with respect to the pristine ZnO. Since the APTMS moiety links through hydroxyl groups to the oxide surface (Zn-OH), leading to Zn-O-SiR bonds, the above-mentioned-observation further confirms the successful amine functionalization of our ZnO NCs.

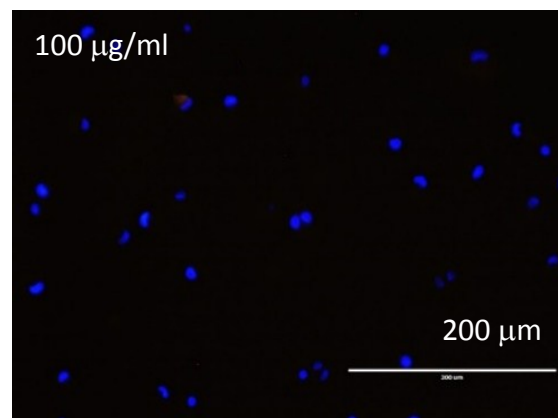
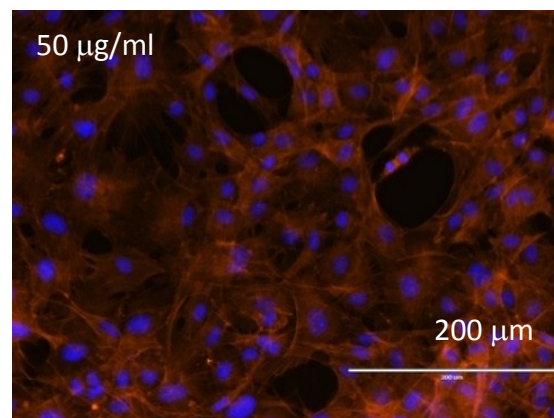
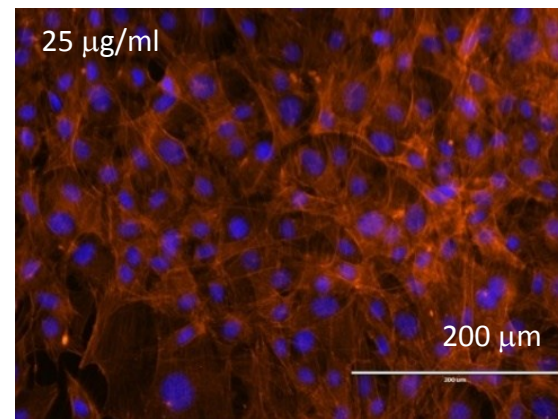
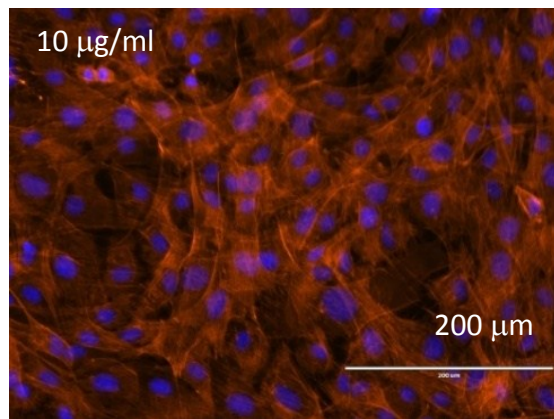
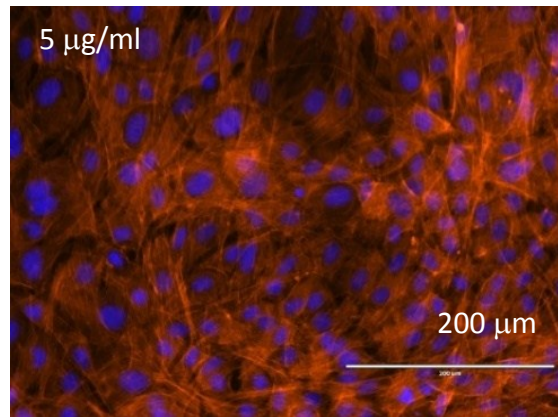
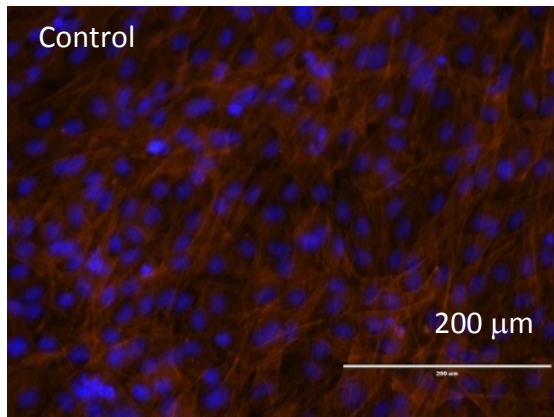


Figure S3. Fluorescent microscope images of pre-osteoblasts cultured up to 70 % of confluence after incubation for 4 days with ZnO NCs at different concentrations.

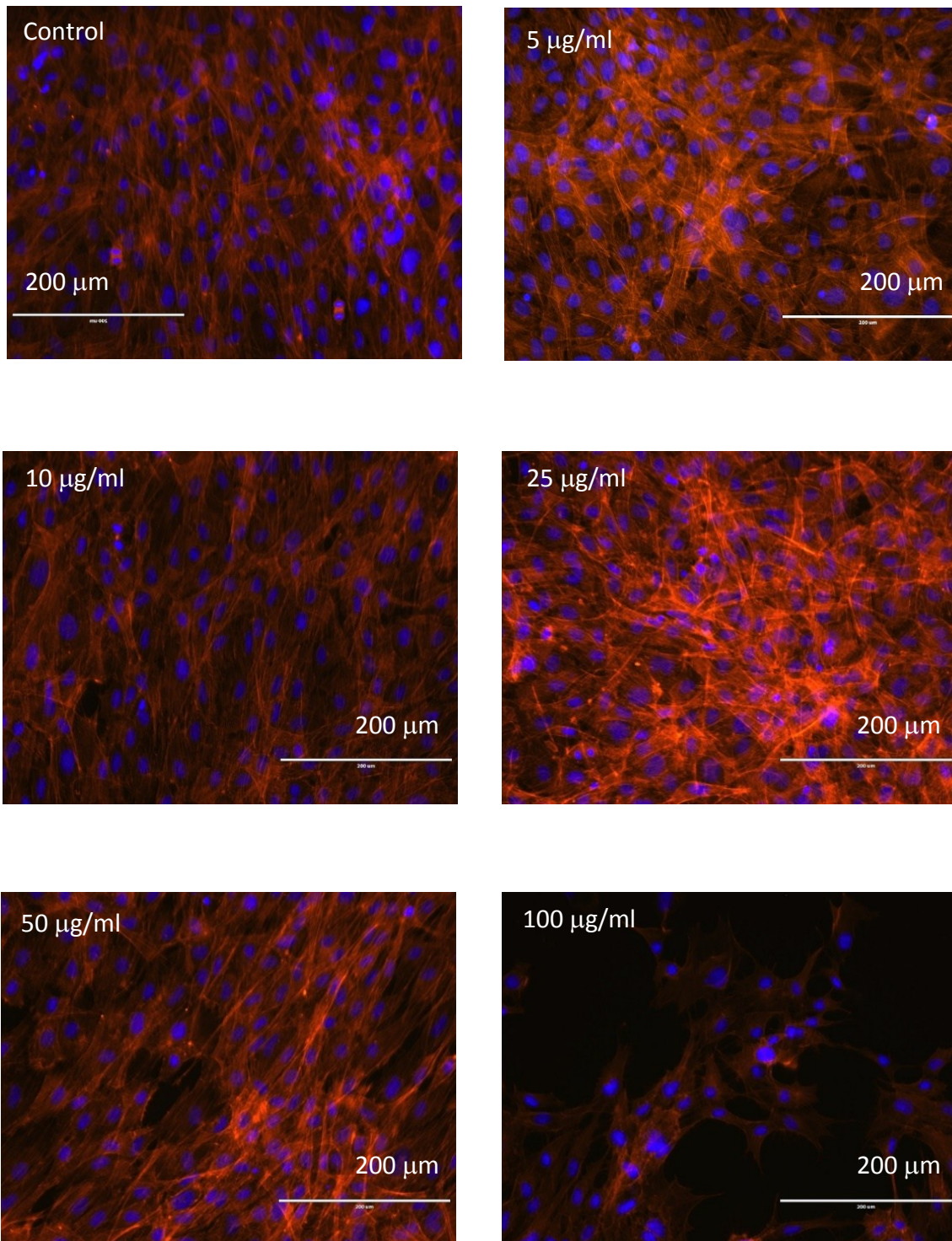


Figure S4. Fluorescent microscope images of pre-osteoblasts cultured up to 70 % of confluence after incubation for 4 days with ZnO-NH₂ NCs at different concentrations.

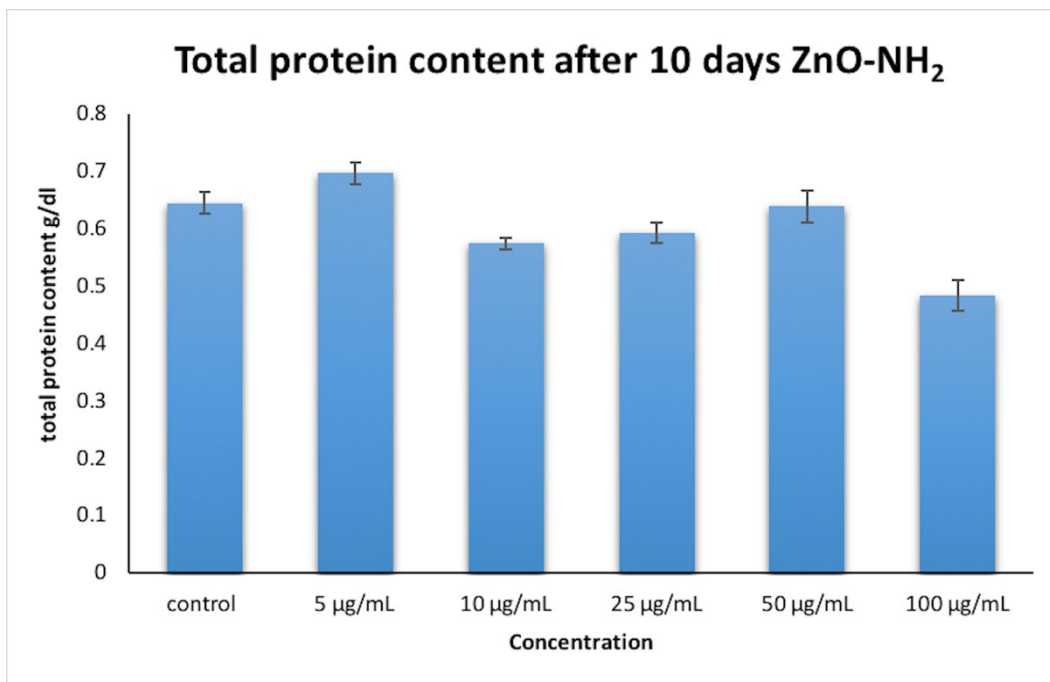
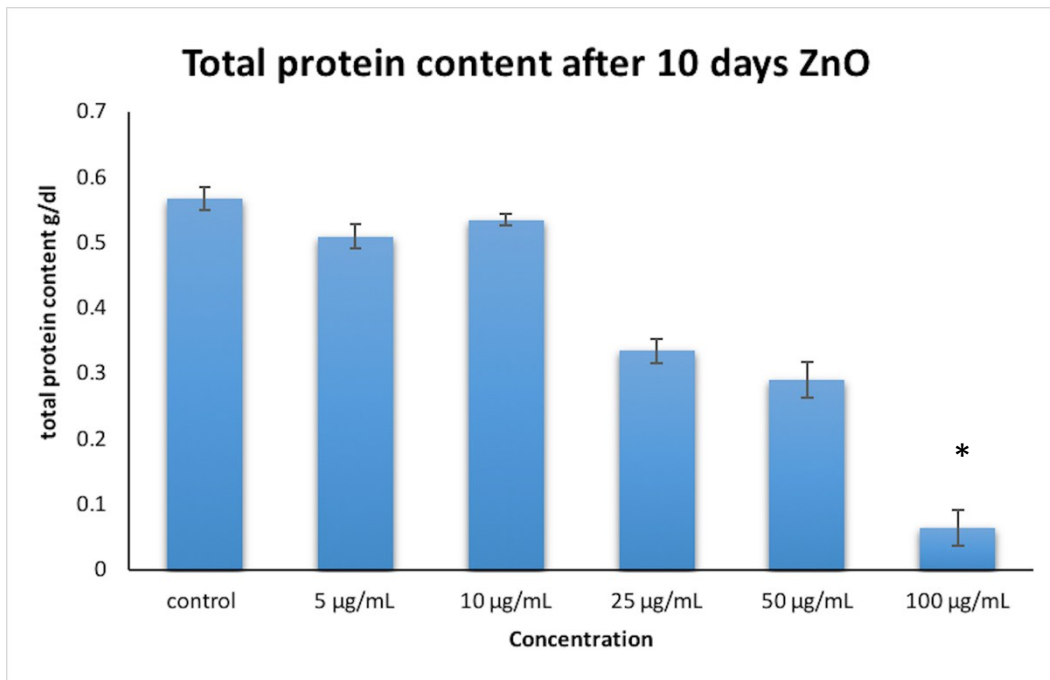


Figure S5. Differentiation assays in term of total protein content after 10 days of incubation with ZnO (top) and ZnO-NH₂ (bottom) NCs at different concentrations. ($p < 0.05$, significant differences compared to control denoted by an asterisk).



Figure S6. Cell morphology evaluation by optical microscopy of MC3T3-E1 pre-osteoblast cells after 10 days of incubation with ZnO NCs.



Figure S7. Cell morphology evaluation by optical microscopy of MC3T3-E1 pre-osteoblast cells after 10 days of incubation with ZnO-NH₂ NCs.

Table S1. Reduction in bacteria viability after 24 h of incubation with ZnO and ZnO-NH₂ NCs, respectively. The values shown in bold indicate a CFU concentration less than 10² CFU/ml, which is considered as positive effectiveness.

Concentration	<i>E. coli</i> vs ZnO	<i>E. coli</i> vs ZnO-NH ₂	<i>S. aureus</i> vs ZnO	<i>S. aureus</i> vs ZnO-NH ₂
5 µg/mL	99.999%	100%	99.923%	99.935%
10 µg/mL	100%	100%	99.965%	99.963%
25 µg/mL	100%	100%	99.985%	99.990%
50 µg/mL	100%	100%	99.940%	99.853%
100 µg/mL	100%	100%	99.963%	99.883%